

***In situ* TEM observation of controlled gold contact failure under electric bias**Yoshifumi Oshima^{1,*} and Yoshihiko Kurui²¹*Research Center for Ultra HVEM, Osaka University, 7-1 Midorigaoka, Ibaraki 567-0047, Japan*²*Department of Condensed Matter Physics, Tokyo Institute of Technology, Oh-okayama, Meguro-ku, Tokyo 152-8551, Japan*

(Received 18 October 2012; revised manuscript received 26 December 2012; published 7 February 2013)

We directly observed the gradual thinning and eventual failure of single-crystalline gold (Au) contacts under increasing electric bias. The contacts fractured in a controlled manner at a current density of around $(2-3) \times 10^{10}$ A/cm², so that nanogaps 1–2 nm wide were formed reproducibly. Also, the surface migration of Au atoms was observed to be enhanced by stretching the contact, suggesting that the surface migration of the Au atoms was sensitive to the stress distribution. The Au contact is probably fractured in a controlled manner, when it becomes stress free.

DOI: [10.1103/PhysRevB.87.081404](https://doi.org/10.1103/PhysRevB.87.081404)

PACS number(s): 73.63.Rt, 68.37.Lp, 68.60.Wm

The failure of metal contacts under an electric bias is an interesting phenomenon from both fundamental and technological points of view. The metal interconnects of the integrated circuits were reported to fail due to the nucleation of voids when the current density exceeded a certain value, which was typically on the order of 10^5 or 10^6 A/cm².^{1,2} On the other hand, a gold (Au) atomic chain did not fail even under an applied bias voltage of 1 V, which corresponds to a current density on the order of 10^{11} A/cm².³⁻⁵ Since electromigration, which is caused by electron scattering at defects in the conductor, does not occur in an Au atomic chain because of a ballistic conductor,⁶ the failure mechanism of the Au atomic chain must be different from the case of the interconnects. Theoretical calculation suggests that current-induced force weakens the atomic bonds among the end atom of the atomic chain and the edge atom of the electrode, resulting in the failure of the atomic chain.⁶

By *in situ* transmission electron microscopy (TEM) observation, Heerdshe *et al.*⁷ found that the cathode side of the gap had a relatively sharp edge, while the anode side was more rounded after breaking polycrystalline Au contacts under electric bias. They suggested that the direct force of the electric field may result in these different electrode shapes after the failure. On the other hand, Strachan *et al.*⁸ directly observed layer-by-layer thinning of a single-crystalline Au nanowire under electric bias and concluded that the current facilitated the thermal excitation of surface atoms, which were then removed by current-induced forces. They clearly show that the thinning process of single-crystalline Au contacts is different from that of polycrystalline Au contacts. But, the final stage of the failure is still open to question. Because, they mentioned that the Au bridge was unstable at the conductance below $5G_0$ (where $G_0 = 2e^2/h$, the quantized unit of conductance, e is the elemental charge, and h is Planck's constant) and the nanogap could be formed without electric bias.^{8,9} It is inconsistent with the fact that the Au atomic contact, which is probably formed at the final stage of breaking a single-crystalline Au contact, is stable even under electric bias as mentioned above. In order to clarify the failure mechanism, it is necessary to directly observe the failure of single-crystalline Au contact under electric bias.

In this study, using an ultrahigh-vacuum TEM combined with a scanning tunneling microscope (TEM-STM), we

directly observed the structural and current evolution of Au contacts while increasing the bias voltage. The Au contacts examined were single crystalline, and were fabricated between the two electrodes of the STM equipment. These Au contacts were found to be ballistic conductors up to $40G_0$. The Au contacts were thinned intermittently above 10 mV and broke at 0.2–0.3 V. The surface migration of Au atoms was enhanced by stretching the contact.

The TEM-STM experiment was done at room temperature using our homemade STM within an ultrahigh-vacuum (UHV) TEM (JEM-2000VF).¹⁰ The base pressure in the TEM was maintained below 1×10^{-7} Pa in order to prevent contamination of the specimen surface, as contamination was observed to resist surface migration of Au atoms under electric bias, resulting in disturbing the thinning process of the Au contacts (not shown). The TEM was operated at an accelerating voltage of 200 kV. The imaging current density was approximately 0.2 pA/nm², which did not influence the electric current passing through the contact.¹⁰ TEM images were taken by a TV camera and captured as an NTSC signal (30 fps). The current measurement had an accuracy of 1% and a measurable limit of 40 pA, and was synchronized with each TEM image using the NTSC trigger signal.¹¹

Single-crystalline Au contacts were fabricated by many cycles of stretching and retracting the contact using the tube piezoactuator of the STM. This is referred to as *mechanical annealing*, and was described by Untiedt *et al.*¹² Figures 1(a) and 1(b) show typical TEM images of Au contacts with their axes along the $\langle 110 \rangle$ and $\langle 111 \rangle$ directions, respectively. These contacts showed $\{111\}$ and/or $\{200\}$ lattice fringes, indicating that they were single crystalline.

The cross-sectional area of the Au contact was required in order to estimate the current density. We assumed that the observed Au contacts were circular, since the Au contacts of the $[110]$ axis, which were fabricated by mechanical annealing, probably had symmetrical hexagonal cross sections.¹³ The cross-sectional area was obtained from the diameter of the contact, which was measured in the TEM image as shown in Figs. 1(a) and 1(b). The conductance was obtained by dividing the current by the bias voltage and normalizing by the quantized unit of conductance, G_0 . Figure 1(c) shows a graph of the conductance of the contact as a function of the cross-sectional area.

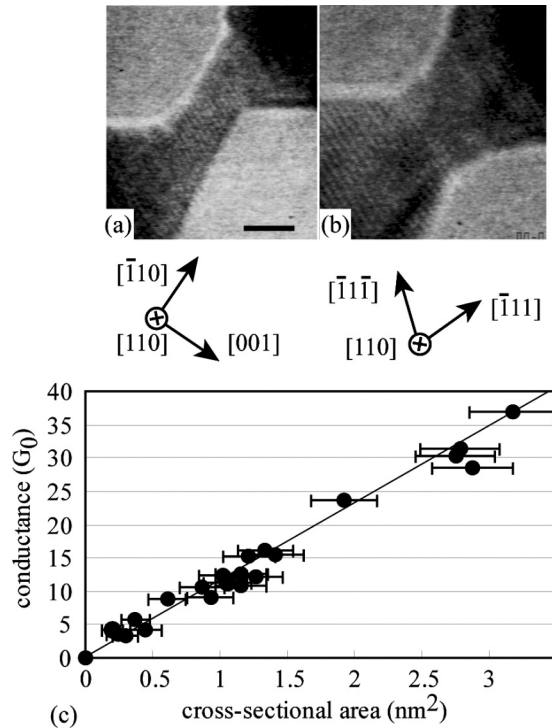


FIG. 1. Typical TEM images of gold (Au) contacts. (a) A hexagonal prism Au contact, which has the axis parallel to the $\langle 110 \rangle$ direction. (b) A bottleneck contact, which has the axis parallel to the $\langle 001 \rangle$ direction. (c) A graph of the conductance of the Au contacts as a function of their cross-sectional area. The cross-sectional area was obtained by assuming that the cross section is a circle. The error bar shows the measurement deviation. The line through the origin represents the Sharvin formula, which is applicable for a ballistic conductor.

Figure 1(c) shows that the measured conductance value is proportional to the cross-sectional area up to $40G_0$. Furthermore, this linear relationship was in agreement with the Sharvin formula,¹⁴

$$G = G_0 * \pi S / \lambda_f^2, \quad (1)$$

where S is the cross-sectional area and λ_f is the electron Fermi wavelength ($=0.52$ nm for gold). This result indicates that the Au contact is a ballistic conductor up to a conductance of $40G_0$. The conductance value is not an exact integral multiple of the quantized unit of conductance, which could be explained by multiple reflections of conduction electrons at the interface between the Au contact and the electrode.¹⁵ In the ballistic regime, the current density is proportional to the bias voltage (V), as expressed by

$$j = GV/S = G_0 * \pi / \lambda_f^2 * V. \quad (2)$$

This means that the current density can be controlled by the bias voltage in the ballistic regime.

Figure 2(a) shows the current evolution as a function of the cross-sectional area when the bias voltage was smoothly increased from 0 at a constant rate. At a bias voltage of 20 mV [indicated by an oval in Fig. 2(a)], the contact was thinned from 3.9 to 3.5 nm^2 in cross section and the current decreased. The current density, which corresponds to the slope of the current evolution and also is proportional to the bias voltage, was 1.5×10^9 A/cm². No contact thinning occurred until the bias

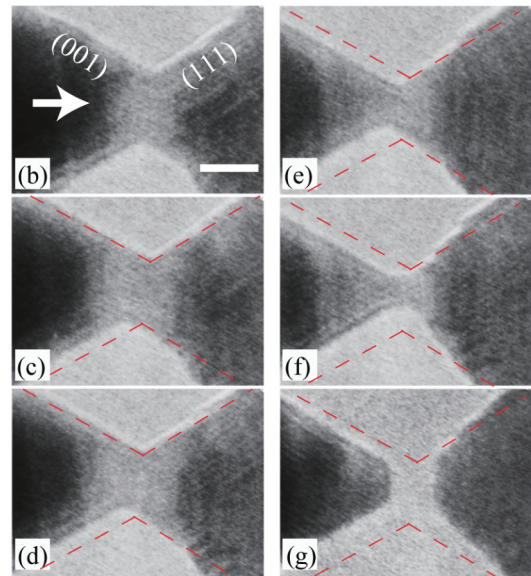
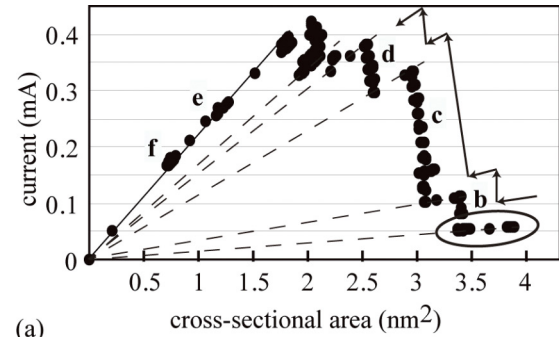


FIG. 2. (Color online) (a) A graph of electric current evolution as a function of the cross-sectional area of an Au contact while the bias voltage was increased. The voltage increased in steps of about 10 mV per 1/2 second. (b)–(g) A series of TEM images taken at locations labeled **b** to **g** in the graph in (a). In the TEM images, the red dashed line (light gray dashed line) represents the shape of the Au contact in the TEM image of (b) drawn to assist in easily distinguishing the shape change. The white arrow indicates the direction of electron flow under electric bias. The white bar corresponds to 2 nm in distance.

voltage of 40 mV and the current increased with increasing the bias voltage. At 40 mV, the contact was thinned from 3.5 to 3 nm^2 and the current decreased. The current density was 3.2×10^9 A/cm². Again, contact thinning did not occur until a bias voltage of 0.13 V. In the process of increasing the bias voltage, the current increases stepwise as indicated by arrows in Fig. 2(a). Finally, the current decreased linearly to zero, indicating that the contact was smoothly growing thinner at the moment of failure. The failure bias voltage was 0.27 V, which corresponds to a current density of 2.4×10^{10} A/cm².

The TEM images shown in Figs. 2(b)–2(f) were taken at locations marked **b** to **f**, respectively, in the current evolution of Fig. 2(a) (see the Supplemental Material for movie S1¹⁶). Electrons flowed from left to right, as indicated by a white arrow in Fig. 2(b) (the negative electrode was at the left side). We observed that Au atoms were migrated along the same direction as the electron flow (see movie S1¹⁶) as reported previously.^{7,8,17} Two (111) surface layers of the negative electrode were removed in Fig. 2(c), as the contact was thinned

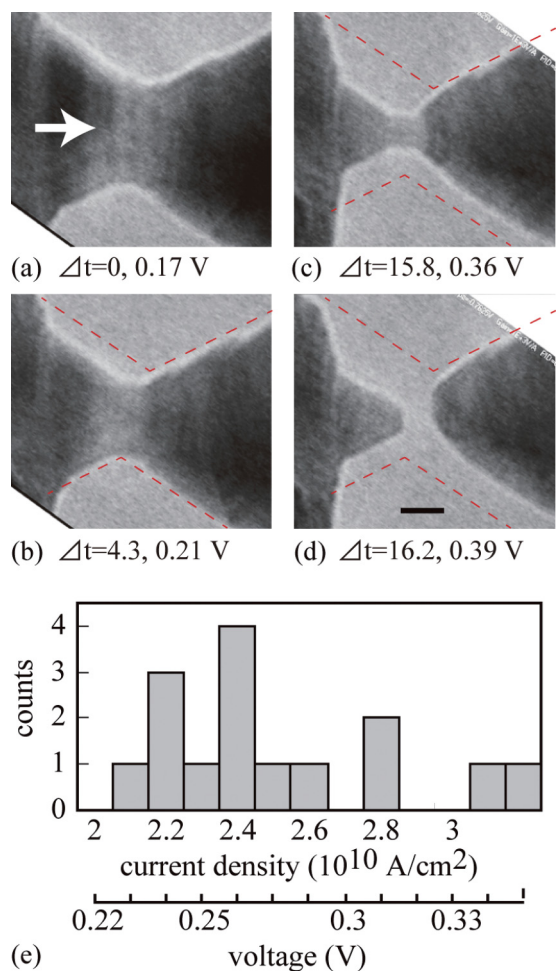


FIG. 3. (Color online) (a)–(d) A series of TEM images of different Au contacts while the bias voltage was increased. In each image, the elapsed time from (a), Δt , and the bias voltage are shown. The red dashed line (light gray dashed line) represents the shape of the Au contact in the TEM image of (a). The white arrow indicates the direction of electron flow under electric bias. The black bar corresponds to 2 nm in distance. (e) A histogram of the current density or bias voltage at the time of failure of the Au contacts.

from 3.5 to 3 nm 2 in cross section. In Fig. 2(d), although the contact was thinned from 3 to 2.5 nm 2 , surface layers were apparently not removed. Surface layers, which are not shown in the TEM image of Fig. 2(d), must be removed at this thinning process. At the moment of failure, two (001) surface layers of the negative electrode were removed, as shown in Fig. 2(e), and subsequently two (111) surface layers of the negative electrode and also two (001) surface layers of the positive electrode were removed, as shown in Fig. 2(f). These images show that the contact was thinned layer-by-layer, right up to the moment of failure. In detail, the surface layers of the negative electrode were more removed than ones of the positive electrode, resulting in asymmetric electrode shapes: The negative electrode evolved a sharp edge, while the positive electrode maintained its initial shape. After failure, a 2 nm nanogap was visible, as shown in Fig. 2(g).

Figure 3 shows a series of TEM images taken during the thinning of another Au contact while increasing the bias voltage (see also movie S2 16). The negative electrode gradually

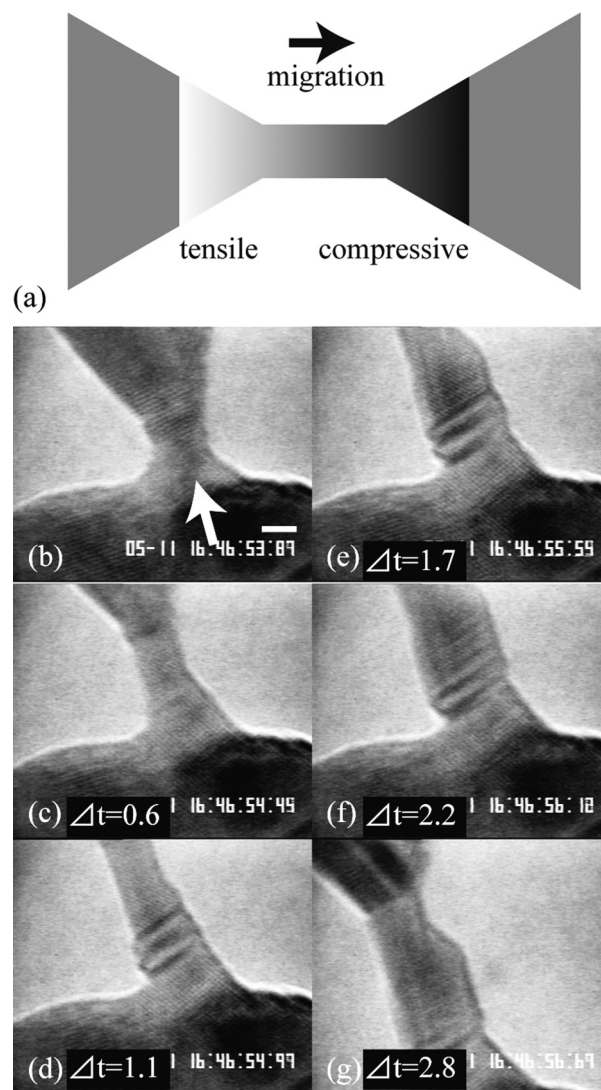


FIG. 4. (a) A schematic illustration of the stress distribution at the contact. The left part is the negative electrode, and the right part is the positive electrode. The black arrow indicates the direction of surface migration and of the electron flow. (b)–(g) A series of TEM images of an Au contact obtained while stretching it along the (111) direction, which was almost parallel to the contact axis, at a rate of 2.3 nm per second under a bias voltage of 0.2 V. In each image, the elapsed time from (a), Δt , is shown. The white arrow indicates the direction of electron flow under electric bias. The white bar corresponds to 1 nm in distance.

shrank, but the positive electrode did not change in size. Obviously, the surface layers of the negative electrode were preferentially removed by the surface migration of Au atoms. After failure, a 1.5 nm nanogap was evident in Fig. 3(d). This process confirms the findings of Fig. 2. Such a controlled manner of thinning was reproducibly observed for 20 different Au contacts under electric bias. Figure 3(e) shows a histogram of the failure current density and bias voltage. We found that the current density (bias voltage) was approximately $(2\text{--}3) \times 10^{10}$ A/cm 2 (0.2–0.3 V) at the time of failure.

We observed that single-crystalline Au contacts were thinned layer-by-layer under electric bias. During the thinning process, the Au contact became a bottlenecked shape which

was suspended between two electrodes surrounded by three {111} and/or {100} facets as reported previously.¹⁸ These observations are the same as mentioned by Strachan *et al.*⁸ (“unzipping model”). Also, we observed that both electrodes were asymmetric in shape at the failure, as shown by Heersche *et al.*⁷ But, we found that very thin Au contacts fractured in a controlled manner even under electric bias, although they were reported to be broken spontaneously under no electric bias in the previous works.^{7–9} This finding is in agreement with the previous result that an Au atomic chain is stable even under electric bias.^{3–5} Since the observed contacts were fabricated by mechanical annealing, they are suggested to be less stressed, which is different from the previously observed contacts.

The failure mechanism of Au contacts has been explained by local heating, current-induced force, and nonthermal process. Local heating including melting or evaporation of Au atoms does not explain the failure of the observed Au contacts, because electrons are not scattered at the ballistic regime of the contact. Based on a theoretical model proposed by Todorov *et al.*,⁶ the temperature of a very thin Au contact (length = 2 nm, bias voltage = 0.3 V) was estimated to be almost the same as room temperature. Experimentally, the current-induced heating was reported to be negligible in Au contacts even under high electric bias.¹⁹ Also, current-induced force,²⁰ which is closely related to the chemical bonding, does not explain the failure. It pushes the atoms towards the negative electrode, which is the opposite direction to the migration of the Au atoms in our observation. In addition, a nonthermal process is not suitable for the origin of the failure. Umeno *et al.*²¹ reported that the conductance of a very thin junction showed successive drops in quantum steps of conductance only when the bias voltage exceeded certain critical values. But, in this observation, as shown in the current curve of Fig. 2, the threshold voltage for thinning the Au contact increases stepwise with decreasing the diameter of the contact.

We believe that electric wind force is generated around the contact, since the Au atoms were observed to be migrated on the surface towards the positive electrode. The conducting electrons seem to transfer momentum to Au atoms via scattering around the interface between the negative electrode

and Au ballistic contact, and also between the contact and positive electrode. They are not scattered in the ballistic contact. As a result, the stress at the left side of the contact and at the positive electrode is relatively compressive as shown in Fig. 4(a), which causes a stress gradient near both interfaces. We believe that the stress gradient suppresses the surface migration of Au atoms towards the positive electrode. This belief is supported by the previous reports: The length of the Au contact was observed to be shortened by 0.4 nm at the bias voltage of 0.25 V,²² suggesting that the compressive stress was generated at the contact region. In addition, in the case of metal interconnects, the compressive stress increased around the interface between the interconnect and positive electrode, causing a stress gradient between the two electrodes and suppressing the migration of Au atoms.^{23,24}

It is difficult to directly detect the stress distribution around the contact. Instead, we observed the structural evolution of an Au contact by stretching it while applying a bias voltage, as shown in Figs. 4(b)–4(g) (see also movie S3¹⁶), since the stress distribution is expected to be changed by stretching. The Au contact grew continuously, since the Au atoms are supplied continuously by the surface migration from the negative electrode to the contact. In this case, the compressive stress is probably diminished by stretching the contact, resulting in enhancement of the surface migration. It indicates that the surface migration of Au atoms is sensitive to the stress distribution at the contact.

In conclusion, we observed the failure of single crystalline gold (Au) contacts, which were ballistic conductors below $40G_0$, by applying the bias voltage at room temperature. Au atoms were always migrated on the surface in the same direction as the electron flow under electric bias. The Au contacts, which were stress free initially, were failed at a current density of $(2–3) \times 10^{10}$ A/cm² in a controlled manner, reproducibly forming a few-nanometer gap. We also observed that the surface migration of Au atoms was enhanced by stretching the contact, suggesting that it was sensitive to the stress distribution at the contact. The failure of the Au contacts under electric bias is probably determined not only by the current density but also by the stress distribution at the contact.

*oshima@uhvem.osaka-u.ac.jp

¹M. Etzion, I. A. Blech, and Y. Komem, *J. Appl. Phys.* **46**, 1455 (1975).

²C. Durkan, M. A. Schneider, and M. E. Welland, *J. Appl. Phys.* **86**, 1280 (1999).

³A. I. Yanson, G. Rubio Bollinger, H. E. van den Brom, N. Agrait, and J. M. van Ruitenbeek, *Nature (London)* **395**, 783 (1998).

⁴H. Yasuda and A. Sakai, *Phys. Rev. B* **56**, 1069 (1997).

⁵K. Itakura, K. Yuki, S. Kurokawa, H. Yasuda, and A. Sakai, *Phys. Rev. B* **60**, 11163 (1999).

⁶T. N. Todorov, J. Hoekstra, and A. P. Sutton, *Phys. Rev. Lett.* **86**, 3606 (2001).

⁷H. B. Heersche, G. Lientschnig, K. O’Neill, H. S. J. van der Zant, and H. W. Zandbergen, *Appl. Phys. Lett.* **91**, 072107 (2007).

⁸D. R. Strachan, D. E. Johnston, B. S. Guiton, S. S. Datta, P. K. Davies, D. A. Bonnell, and A. T. Charlie Johnson, *Phys. Rev. Lett.* **100**, 056805 (2008).

⁹D. R. Strachan, D. E. Smith, D. E. Johnston, T.-H. Park, and Michael J. Therien, *Appl. Phys. Lett.* **86**, 043109 (2005).

¹⁰Y. Oshima, K. Mouri, H. Hirayama, and K. Takayanagi, *Surf. Sci.* **531**, 209 (2003).

¹¹Y. Oshima, *J. Electron Microsc.* **61**, 133 (2012).

¹²C. Untiedt, G. Rubio, S. Vieira, and N. Agrait, *Phys. Rev. B* **56**, 2154 (1997).

¹³Y. Kurui, Y. Oshima, and K. Takayanagi, *J. Phys. Soc. Jpn.* **76**, 123601 (2007).

¹⁴Y. V. Sharvin, *Zh. Eksp. Teor. Fiz.* **48**, 984 (1965).

¹⁵Y. Kurui, Y. Oshima, M. Okamoto, and K. Takayanagi, *Phys. Rev. B* **79**, 165414 (2009).

¹⁶See Supplemental Material at <http://link.aps.org/supplemental/10.1103/PhysRevB.87.081404> for the corresponding movies.

¹⁷T. Kizuka, S. Kodama, and T. Matsuda, *Nanotechnology* **21**, 495706 (2010).

- ¹⁸Y. Oshima, Y. Kurui, and K. Takayanagi, *J. Phys. Soc. Jpn.* **79**, 054702 (2010).
- ¹⁹M. Tsutsui, Y.-k. Taninouchi, S. Kurokawa, and A. Sakai, *Jpn. J. Appl. Phys.* **44**, 5188 (2005).
- ²⁰M. Brandbyge, K. Stokbro, J. Taylor, J.-L. Mozos, and P. Ordejón, *Phys. Rev. B* **67**, 193104 (2003).
- ²¹A. Umeno and K. Hirakawa, *Appl. Phys. Lett.* **94**, 162103 (2009).
- ²²M. Yoshida, Y. Oshima, and K. Takayanagi, *Appl. Phys. Lett.* **87**, 103104 (2005).
- ²³I. A. Blech, *J. Appl. Phys.* **47**, 1203 (1976).
- ²⁴P. C. Wang, I. C. Noyan, S. K. Kaldor, J. L. Jordan-Sweet, E. G. Liniger, and C. K. Hu, *Appl. Phys. Lett.* **76**, 3726 (2000).